Theoretical and experimental investigation of strongly localized plasmons on triangular metal wedges for subwavelength waveguiding

D. F. P. Pile[a] and T. Ogawa
Department of Optical Science and Technology, Faculty of Engineering, The University of Tokushima, Minamijosanjima 2-1, Tokushima 770-8506, Japan

D. K. Gramotnev
Applied Optics Program, School of Physical and Chemical Sciences, Queensland University of Technology, GPO Box 2434, Brisbane, QLD 4001, Australia

T. Okamoto, M. Haraguchi, and M. Fukui
Department of Optical Science and Technology, Faculty of Engineering, The University of Tokushima, Minamijosanjima 2-1, Tokushima 770-8506, Japan

S. Matsuo
Department of Ecosystem Engineering, Graduate School of Engineering, The University of Tokushima, Minamijosanjima 2-1, Tokushima 770-8506, Japan

(Received 22 April 2005; accepted 7 June 2005; published online 3 August 2005)

We report numerical analysis and experimental observation of strongly localized plasmons guided by a triangular metal wedge. Dispersion and dissipation of such wedge plasmons are analyzed using the finite-difference time-domain algorithm. Experimental observation is conducted by the end-fire excitation and near-field detection of the predicted plasmons on a 40° silver nanowedge. Good agreement with the theoretically predicted propagation distances is demonstrated. Differences between the theoretical and experimental field distribution are explained by insufficient resolution of the near-field optical probe. © *2005 American Institute of Physics*. [DOI: 10.1063/1.1991990]

The diffraction limit of light[1–3] is a major obstacle on the way of achieving high degree of miniaturization and integration of optical devices and circuits. The main approach to overcome this problem is related to use of surface plasmons in metallic nanostructures, such as rectangular metallic nanostrips,[4–6] nanorods,[3,7] nanochains,[1,2,8] metallic gaps,[9] trapezium-like nanowedges,[10] etc. Parabolic metal wedges[11] could also be used for the design of subwavelength waveguides, though such a possibility has not been specifically analyzed. Recently, a new type of strongly localized plasmon—channel plasmon-polariton (CPP)—has been investigated theoretically in metallic grooves.[12–16] The major features of CPPs in V grooves include a unique combination of strong localization and relatively low dissipation,[13,14] single-mode operation,[14] possibility of nearly 100% transmission through sharp bends,[15] and high tolerance to structural imperfections.[16]

Only very few experimental attempts to investigate different types of plasmonic waveguides with subwavelength localization have been undertaken so far.[2,6,10] It has been shown that nanochain waveguides have very strong dissipation and short propagation distances ($\lesssim$200 nm).[1,2,8,17] Rectangular nanostrip waveguides have significantly lower dissipation,[5,6] but the experimentally achieved plasmon localization was only just below the diffraction limit.[6] No experimental investigation of gap plasmon waveguides, CPPs or parabolic wedge modes has been undertaken so far.

Therefore, the aim of this letter is in numerical analysis and experimental observation of new strongly localized plasmons guided by triangular metal wedges.

The numerical analysis is carried out by means of the three-dimensional (3D) finite-difference time-domain (FDTD) algorithm[13–16] and the compact-two-dimensional (compact-2D) FDTD approach.[18,19] The latter has been extended to plasmonic waveguides with negative permittivity[19] by using the local Drude model.[13–16,20] The compact-2D FDTD algorithm appears to be highly efficient, and provides more accurate field distribution and wave vectors of guided plasmons. However, it cannot be used for irregular guides with bends, nonuniformities, etc. Therefore, we will be using both of the FDTD formulations.

The analyzed structure with a silver wedge of the angle θ and a rectangular aperture is presented in Fig. 1(a). Plasmons in this structure are generated by means of the end-fire excitation using a bulk wave with the electric field parallel to the z-axis, incident onto the end of the wedge at an angle 45° [Fig. 1(a)]. The aperture is used to suppress scattered bulk waves and surface plasmons on the sides of the wedge.

In the absence of the aperture, the steady-state instantaneous field distribution along the wedge in the (x,z) plane, calculated using the 3D FDTD algorithm, displays a snake-like pattern of beats localized near the tip of the wedge [Fig. 1(b)]. The strongly localized periodic field along the tip suggests the existence of a new type of localized plasmonic eigenmode—wedge plasmon (WP). The snake-like pattern is produced by interference of the WP and the surface plasmons on the sides of the wedge. This is confirmed by the Fourier analysis of the field at the tip.[13,14] Two distinct maximums in the Fourier spectrum of the field are obtained in Fig. 1(b) at the wave numbers $q_1 \approx 1.20\times10^7$ m^{-1} (WP) and $q_0 \approx 1.025\times10^7$ m^{-1} (surface plasmon at the silver-vacuum interface). This also suggests that the considered wedge supports only one (fundamental) WP mode. Higher modes would have produced more maximums in the Fourier spectrum, and this indeed happens when $\theta \leqslant 30°$.

Generation of surface plasmons and WP occurs at the point of the end-fire excitation. Beyond this point, surface

[a]Electronic mail: pile@opt.tokushima-u.ac.jp and d.pile@qut.edu.au

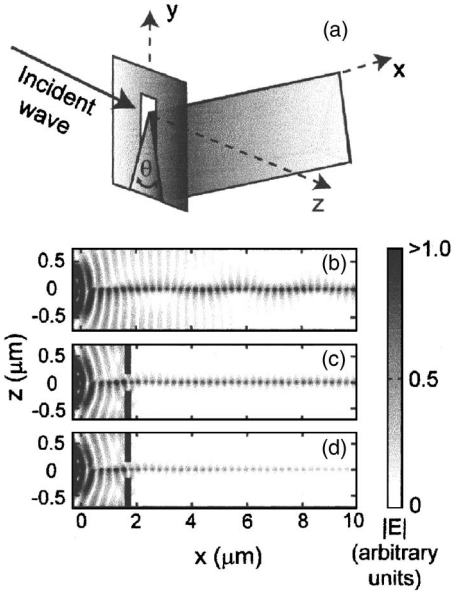

FIG. 1. (a) A triangular silver wedge with the end-fire excitation of WP modes through an aperture for suppression of surface and bulk waves. The aperture in a ~200-nm-thick silver film is ≈300 nm wide (along the z axis) and its top edge is ≈170 nm above the tip of the wedge; the aperture is placed on the wedge at the distance ≈1.6 μm from its end (i.e., from the point of the end-fire excitation). (b)–(d) Distributions of the magnitude of the electric field in the (x,z) plane, calculated using the 3D FDTD method for the silver wedge with the angle $\theta=40°$ in vacuum at the vacuum wavelength $\lambda_{vac}=0.6328$ μm (He–Ne laser). (b) No aperture and no dissipation in the metal; the metal permittivity: $\varepsilon_m=-16.22$. (c) In the presence of the aperture and in the absence of dissipation. (d) In the presence of both the aperture and dissipation: $\varepsilon_m=-16.22+0.52i$. The presented metal permittivities were determined using the local Drude model[19,20] with the electron charge density $\rho\approx-7.684\times10^9$ C/m^3 and damping frequency $f_d=0$ Hz [for (b,c)], and $f_d\approx1.4332\times10^{13}$ Hz [for (d)].

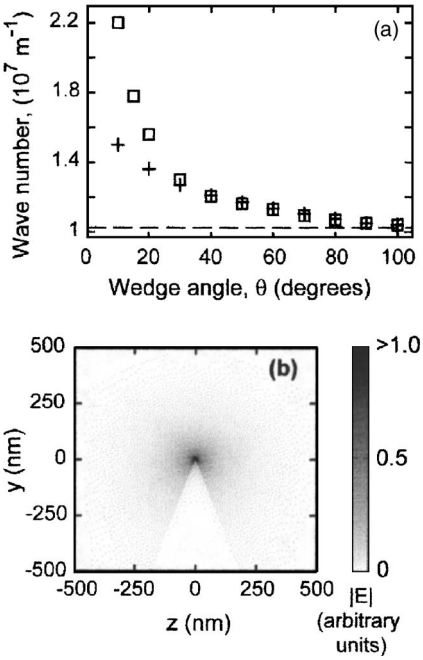

FIG. 2. (a) The dependencies of the wave number of the fundamental WP mode on wedge angle θ, calculated by 3D FDTD (crosses) and compact-2D FDTD (squares). The horizontal dashed line represents the wave number $q_0=1.025\times10^7$ m^{-1} of the surface plasmons on the sides of the wedge. (b) The distribution of the magnitude of the electric field (compact-2D FDTD) in a cross section perpendicular to the tip of the wedge. The structural and wave parameters are the same as for Fig. 1.

plasmons experience significant diffractional divergence. Therefore, if we place a small aperture onto the wedge at some distance from the point of the end-fire excitation, so that it blocks the diverged surface plasmons and lets only WP through, this should significantly reduce the beats-Fig. 1(c). Significant presence of scattered bulk and surface waves can be seen between the end of the wedge and the aperture [$0<x<1.6$ μm, Fig. 1(c)], whereas behind the aperture only the strongly localized WP propagates along the tip of the wedge. The Fourier analysis of the field at the tip behind the aperture shows that the maximum due to surface plasmons disappears from the spectrum.

Figure 1(d) shows the effect of dissipation on WP. It can be determined that the intensity of the WP drops e times within the propagation distance $L_{\text{theory}}\approx2.25$ μm which is noticeably larger than the wavelength of the plasmon and thus is sufficient for a range of nano-optics applications.[1,6,10]

The analysis of the end-fire excitation can only be conducted using the 3D FDTD algorithm. At the same time, the compact-2D FDTD provides more accurate results for the field distribution and dispersion of localized plasmons.[19] The dependencies of the WP wave number on θ for a silver wedge in vacuum, obtained in the compact-2D and 3D FDTD formulations, demonstrate significant differences at $\theta<30°$ [Fig. 2(a)]. This is due to low accuracy and efficiency of 3D FDTD at small θ.

Note that WP modes can only exist if θ is less than a critical angle $\theta_c\approx102°$ [Fig. 2(a)]. If $\theta=\theta_c$, then $q_1=q_0\approx1.025\times10^7$ m^{-1}, and the WP has infinite penetration depth (zero localization) along the sides of the wedge. If $\theta>\theta_c$, WP does not exist as a structural eigenmode, since it leaks into surface plasmons. This is similar to the existence of the upper critical angle for CPP modes in metallic grooves.[13–16]

An example of the field distribution in the fundamental WP mode in a cross section of the 40° silver wedge is presented in Fig. 2(b) demonstrating strong subwavelength localization within the region of ~50 nm.

The experimental observation of WPs were undertaken in the structure shown in Fig. 3(a). An ~1.3 μm silver film was evaporated onto a glass substrate. Four wedges with the height ~1 μm and the radii of about 25 nm were fabricated in this film using the focused-ion beam lithography (FIB). Direct end-fire excitation of WP modes by a laser beam focused onto the end of a wedge led to significant interference of the scattered field with the WP field registered by a near-field scanning optical microscope (NSOM). In addition, drift of the laser beam tightly focused onto the wedge end resulted in substantial fluctuations of the intensity. Therefore, the end-fire excitation was achieved through microholes fabricated in the silver film by means of FIB in front of the wedges [Fig. 3(a)]. A laser beam illuminates the holes from underneath the film. Tight focusing is not required, since the incident and WP fields are separated by the film.

The aperture of the NSOM probe tip was ≈100 nm diameter with ~100 nm aluminum coating. The tip-to-sample distance during measurements was maintained at ≈10 nm by the shear force feedback. The near-field intensities of the generated WPs on the four wedges [Fig. 3(a)] are shown in Fig. 3(b). It can be seen that the intensity of the optical signal registered by NSOM decays along the positive x direction in a similar fashion for all wedges [Fig. 3(b)]. The solid curve in Fig. 3(c) represents the experimentally measured intensity of the NSOM signals along the wedge located at $z=0$ in Fig. 3(b). Its comparison with the theoretical dependence ob-

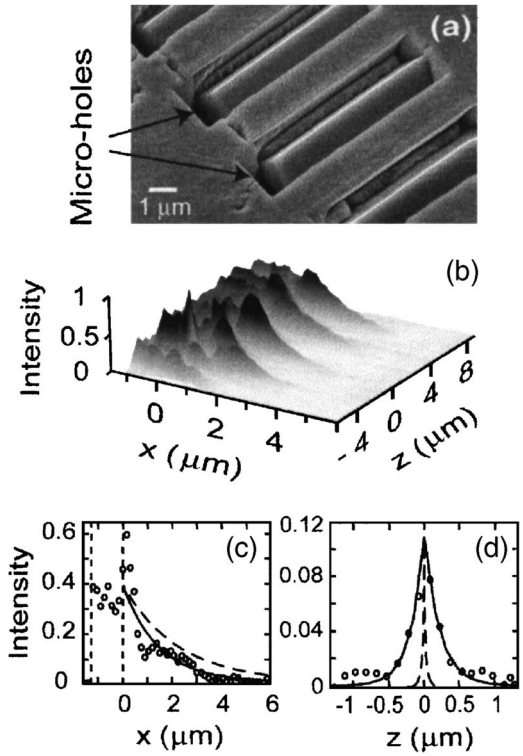

FIG. 3. (a) Scanning electron microscopy image of the experimental structure with four wedges of ≈ 7 μm length in the silver film. (b) NSOM intensity of the optical signal along the four wedges (the x axis is parallel to the wedges). The structure is excited by a beam ($\lambda_{vac}=0.6328$ μm) of circular polarization incident onto the microholes (-1.2 $\mu m < x < 0$ μm) from underneath the silver film [Fig. 3(a)] at an angle of 45° to the x axis. The point of the end-fire excitation: $x=0$. (c) NSOM intensity of the optical signal along the tip of the 40° wedge [at $z=0$ in Fig. 3(b)] with the exponential fit to the experimental points (solid curve) in the waveguide region. The region of the microaperture is shown by the two vertical dotted lines. Dashed curve: theoretical dependence from 3D FDTD. (d) NSOM detected intensity of the optical signal vs z coordinate taken at $x \approx 3$ μm with the distance from the sample surface to the NSOM tip maintained at ≈ 10 nm. Solid curve: exponential fit to the experimental points. Dashed curve: theoretical distribution from the compact-2D FDTD.

tained from the 3D FDTD formulation [dashed curve in Fig. 3(c)] shows that the experimental propagation distance for WP (at the $1/e$ level of its intensity) $L_{exp} \approx 1.5$ μm is smaller than the predicted theoretical value $L_{theory}=2.25$ μm. This can be explained by nonuniformities of the wedge near the tip, which results in additional radiative energy losses. Another reason for this discrepancy may be larger dissipation in the silver film compared to the bulk metal, and the effect of FIB lithography on the optical properties of silver. Taking this into account, the agreement between the theory and experiment [Fig. 3(c)] is good.

Figure 3(d) shows the intensity of the optical signal registered by NSOM when scanning perpendicular to the wedge at the distance $x=3$ μm from the point of excitation (solid curve). For comparison, the corresponding theoretical dependence is also presented (dashed curve). The substantial difference between these dependencies is explained by the low resolution of NSOM tip (with an aperture of ~ 100 nm). In addition, this aperture is surrounded by the 100 nm Al coating, which may result in substantial perturbation of the WP field and distortion of the experimental results. Therefore, only the experimental dependencies of the decaying field along the wedge can be regarded reliable. However, the fact that NSOM has shown lateral localization of the field near the tip of the wedge in the region of ~ 300 nm [Fig. 3(d)] constitutes another proof that WP modes have been successfully detected. This is because such a field distribution is not possible due to bulk or surface waves, which would have experienced strong diffractional divergence.

In summary, this letter has reported the numerical analysis and the first experimental observation of a new type of strongly localized plasmons propagating along the tip of a triangular metal wedge. Plasmon parameters and field structure were determined by means of two different FDTD formulations. In particular, it has been shown that WP modes do not exist if the wedge angle is larger than a critical angle (which for a silver wedge in vacuum and $\lambda_{vac}=0.6328$ μm is $\approx 102°$). Strong subwavelength localization of WP modes has been demonstrated, and reasonable propagation distances have been predicted, which makes WP modes a good candidate for the design of subwavelength plasmonic waveguides.

The first direct excitation of a nanowaveguide by bulk waves was successfully conducted. The predicted and experimentally observed propagation distances are sufficient for the design of nano-scale interconnectors between nano-optical devices. Further increase of the propagation distances could be achieved by means of gain-assisted propagation (which could be achieved by surrounding the metal with a gain medium, as was proposed for surface plasmons).[21]

The authors gratefully acknowledge support from the Japan Society for the Promotion of Science and the High Performance Computing Division at the Queensland University of Technology.

[1] J. R. Krenn, Nat. Mater. **2**, 210 (2003).
[2] S. A. Maier, P. G. Kik, H. A. Atwater, S. Meltzer, E. Harel, B. E. Koel, and A. A. G. Requicha, Nat. Mater. **2**, 229 (2003).
[3] J. Takahara, S. Yamagishi, H. Taki, A. Morimoto, and T. Kobayashi, Opt. Lett. **22**, 475 (1997).
[4] P. Berini, Phys. Rev. B **63**, 125417 (2001).
[5] B. Lamprecht, J. R. Krenn, G. Schider, H. Ditlbacher, M. Salerno, N. Felidj, A. Leitner, and F. R. Aussnegg, Appl. Phys. Lett. **79**, 51 (2001).
[6] J. R. Krenn, B. Lamprecht, H. Ditlbacher, G. Schider, M. Salerno, A. Leitner, and F. R. Aussenegg, Europhys. Lett. **60**, 663 (2002).
[7] C. A. Pfeiffer, E. N. Economou, and K. L. Ngai, Phys. Rev. B **10**, 3038 (1974).
[8] J. R. Krenn, A. Dereux, J. C. Weeber, E. Bourillot, Y. Lacroute, J. P. Goudonnet, G. Schider, W. Gotschy, A. Leitner, F. R. Aussenegg, and C. Girard, Phys. Rev. Lett. **82**, 2590 (1999).
[9] K. Tananka and M. Tanaka, Appl. Phys. Lett. **82**, 1158 (2003); K. Tananka, M. Tanaka, and T. Sugiyama, Opt. Express **13**, 256 (2005); B. Wang and G. P. Wang, Appl. Phys. Lett. **85**, 3599 (2004); B. Wang and G. P. Wang, Opt. Lett. **29**, 1992 (2004).
[10] T. Yatsui, M. Kourogi, and M. Ohtsu, Appl. Phys. Lett. **79**, 4583 (2001).
[11] A. D. Boardman, G. C. Aers, and R. Teshima, Phys. Rev. B **24**, 5703 (1981).
[12] I. V. Novikov and A. A. Maradudin, Phys. Rev. B **66**, 035403 (2002).
[13] D. F. P. Pile and D. K. Gramotnev, Opt. Lett. **29**, 1069 (2004).
[14] D. K. Gramotnev and D. F. P. Pile, Appl. Phys. Lett. **85**, 6323 (2004).
[15] D. F. P. Pile and D. K. Gramotnev, Opt. Lett. **30**, 1186 (2005).
[16] D. F. P. Pile and D. K. Gramotnev, Appl. Phys. Lett. **86**, 161101 (2005).
[17] S. A. Maier, M. L. Brongersma, and H. A. Atwater, Appl. Phys. Lett. **78**, 16 (2001).
[18] A. Asi and L. Shafai, Electron. Lett. **28**, 1451 (1992); A. Cangellaris, IEEE Microw. Guid. Wave Lett. **3**, 3 (1993); M. Qui, Microwave Opt. Technol. Lett. **30**, 327 (2001).
[19] D. F. P. Pile, Appl. Phys. B (accepted for publication).
[20] D. Fowers, Masters thesis, University of Utah, Salt Lake City, Utah, 1994; D. Christensen and D. Fowers, Biosens. Bioelectron. **11**, 667 (1996).
[21] M. P. Nazhad, K. Tetz, and Y. Fainman, Opt. Express **12**, 4072 (2004).